High-accuracy optical clocks with sensitivity to the fine-structure constant variation based on Sm^{10+}

Saleh O. Allehabi[1], V. A. Dzuba[2], and V. V. Flambaum[2]
[1]*Department of Physics, Faculty of Science, Islamic University of Madinah, Madinah 42351, KSA and*
[2]*School of Physics, University of New South Wales, Sydney 2052, Australia*
(Dated: April 10, 2024)

We identify two metastable excited states in Sm^{10+} highly charged ion as candidates for high accuracy optical clocks. Several atomic properties relevant to optical clock development are calculated using relativistic many-body methods. This includes energy levels, transition amplitudes, lifetimes, scalar polarizabilities, black body radiation shift, and the sensitivity to the fine structure constant variation. We found that the clock transitions are not sensitive to perturbation, e.g., relative black body radiation shifts are $\sim 10^{-19}$. The enhancement factor for the α variation is ~ 0.8 for one clock transition and ~ 16 for another.

I. INTRODUCTION

In recent times, there has been significant progress in the accuracy of frequency measurements in optical clock transitions of various atomic systems, including Sr, Yb, Al^+, Hg, Hg^+, and Yb^+. The fractional precision of these measurements has reached a remarkable level of 10^{-18} [1–10]. This progress has led to increased interest in finding clock transition which combine high accuracy of the measurements with high sensitivity to the manifestations of new physics, such as e.g. the variation of the fundamental constants and dark matter which may produce this variation.

Highly charged ions (HCI) have been proposed as a way to search for optical transitions that are sensitive to fine structure constant variations over time [11]. HCI can be used to measure the relative change of the clock frequencies which then can be translated to the time variation of the fine structure constants thereby revealing new physics [12–14]. The key to find optical transitions in HCI sensitive to variation of the fine structure constant is *level crossing* (when energies of the states are considered as functions of the ionisation degree). Highest sensitivity can be found in ions with high Z and ionisation degree Z_i in transitions which in single-electron approximation can be considered as $s-f$ or $p-f$ transitions [11]. The search for such transitions is now a popular area of research (see e.g. reviews [15, 16]).

The Sm^{+10} ion is examined in this work as a potential candidate for next-generation atomic clock. The ion has several advantages. Two excited metastable states are considered as clock states (see Fig. 1). Corresponding transitions between ground and metastable states have different sensitivity to the variation of the fine structure constant because one is the transition between states of the same configuration while the other correspond to the $p-f$ single-electron transition. A change of fine-structure constant can be monitored by measuring one frequency versus another over long period of time. Samarium has seven stable isotopes, five of which have no nuclear spin, which makes it ideal for studying King plot nonlinearities. For a study of this kind, at least four stable isotopes and two transitions with potentially high accuracy of measurements are required. This may lead to useful information about nuclear structure, and limit the strength of new interactions mediated by scalar bosons [17–19]. The transitions are not sensitive to external perturbations, e.g. the relative blackbody radiation shift (BBR) is small, $\sim 10^{-19}$ and can be further suppressed by combining two frequencies [20].

The calculations of this work were performed using the configuration interaction with single-double coupled clusters (CI+SD) [21] method and the configuration interaction with perturbation theory (CIPT) [22] method. We calculated energy levels, Landé g-factors, transition amplitudes between low-lying states, quadrupole moments, and clock state lifetimes. For the estimation of the blackbody radiation shifts of clock frequencies, we also calculated the scalar polarizabilities of the ground and excited clock states. We also calculated the sensitivity of the clock transitions to the variation of the fine structure constant.

II. METHOD

A. Calculation of energy levels

The ground state configuration of Sm^{10+} ion is $[Pd]5s^25p4f^3$. We consider it as a system with Pd-like closed-shell core with six valence electrons above it. Thus, we atribute the $5s$ electrons to the valence space. We use a combination of configuration interaction (CI) with linearized single-double coupled cluster (SD) methods [21]. The calculations are performed using the V^{N-M} approximation [23], where N is the total number of electrons and M is the number of valence electrons ($N = 46$, $M = 6$ in our case). The initial relativistic Hartree-Fock (RHF) procedure is done for the Pd-like closed-shell Sm^{16+} ion. The RHF Hamiltonian includes Breit interaction and quantum electrodynamic (QED) corrections,

$$\hat{H}^{\rm RHF} = c\boldsymbol{\alpha}\cdot\mathbf{p} + (\beta-1)mc^2 + V_{\rm nuc}(r) + V_{\rm core}(r) + V_{\rm Breit}(r) + V_{\rm QED}(r), \quad (1)$$

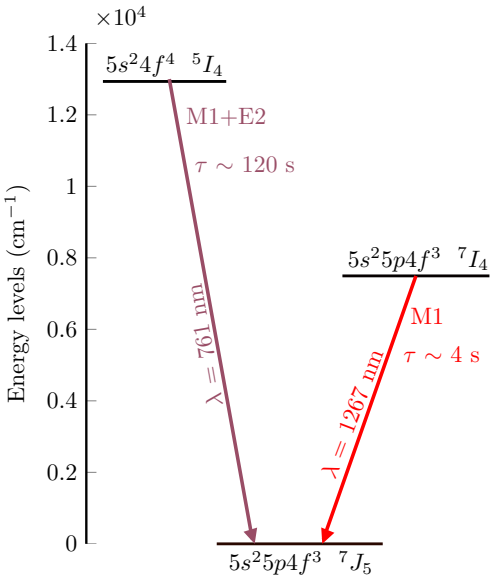

FIG. 1. The first three states of the Sm^{10+} ion. Both excited states are metastable and corresponding transitions to the ground state are considered as clock transitions. Dominating contributions are indicated by symbols M1 (magnetic dipole) and E2 (electric quadrupole). Note that the M1 contribution to the transition at $\lambda = 761$ nm is strongly suppressed due to the difference in leading configurations. Therefore, the electric quadrupole also gives significant contribution.

where c is the speed of light, $\boldsymbol{\alpha}$ and β are the Dirac matrices, $\boldsymbol{p}$ is the electron momentum, m is the electron mass, $V_{\rm nuc}$ is the nuclear potential obtained by integrating the Fermi distribution of the nuclear charge density, $V_{\rm core}(r)$ is the self-consistent RHF potential created by the electrons of the closed-shell core, $V_{\rm Breit}(r)$ is Breit potential [24], $V_{\rm QED}(r)$ is a model QED potential [25].

After completing the self-consistent procedure for the core, the B-spline technique [26, 27] is used to create a complete set of single-electron wave functions. The functions are constructed as linear combinations of B-splines, which are eigenstates of the RHF Hamiltonian. We use 40 B-splines of order 9 in a box with a radius of $R_{\rm max} = 40a_B$; the orbital angular momentum $0 \leq l \leq 6$. These basis states are used to solve the SD equations for the core and for the valence states [21] and for constracting the many-electron basis states for the CI calculations.

Solving the SD equations gives us two correlation operators, Σ_1 and Σ_2. Σ_1 describes the correlation interaction between a particular valence electron and the core, whereas Σ_2 describes the Coulomb interaction screening between a pair of valence electrons [23, 28, 29].

The effective CI+SD Hamiltonian has the form

$$\hat{H}^{\rm CI} = \sum_{i=1}^{M} \left(\hat{H}^{\rm RHF} + \Sigma_1\right)_i + \sum_{i<j}^{M} \left(\frac{e^2}{|r_i - r_j|} + \Sigma_{2ij}\right) \quad (2)$$

Here i and j enumerate valence electrons, summation goes over valence electrons, e is the electron charge, and r is the position operator of the electrons.

There is a well-known fact that increasing the number of valence electrons exponentially increases the size of the CI matrix. We have six valence electrons, resulting in a matrix with an exceptionally large size. It will require considerable computational power to handle such matrix. In exchange for some accuracy, the size of the CI matrix can be reduced by orders of magnitude by using the CIPT (configuration interaction with perturbation theory) method suggested in [22]. By dividing many-electron basis states into two large groups, low-energy states and high-energy states and ignoring the off-diagonal matrix elements between high-energy states the CI equations can be reduced to

$$\langle i|H^{\rm eff}|j\rangle = \langle i|H^{\rm CI}|j\rangle + \sum_k \frac{\langle i|H^{\rm CI}|k\rangle\langle k|H^{\rm eff}|j\rangle}{E - E_k}. \quad (3)$$

Here, $H^{\rm CI}$ is given by (2), $i, j \leqslant N_{\rm eff}$, $N_{\rm eff} < k \leqslant N_{\rm total}$, $N_{\rm eff}$ is the number of low-energy states and $N_{\rm total}$ is the total number of many-electron basis states. Note that the chose of $N_{\rm eff}$ is arbitrary. One can increase it until the results are stable. In our calculations $N_{\rm eff} \sim 10^4$ and $N_{\rm total} \sim 10^7$.

Parameter E in (3) is the energy of the state of interest, and E_k denotes the diagonal matrix element for high-energy states, $E_k = \langle k\,|H^{\rm CI}|\,k\rangle$. The summation in (3) runs over all high-energy states. Note that the parameter E in the denominator of (3) is the same as the energy of the state of interest which is to be obtained from solving the CI equations. Since this energy is not known in advance, iterations over E are needed to find it. More detailed explanations of the technique can be found in Ref. [22].

Knowing the values of the state's g-factors together with their energies, total angular momentum (J) and parity is very useful for the states identification. Therefore, we calculate the g-factors as an expectation value of the magnetic dipole (M1) operator. Comparing the result with the non-relativistic expression

$$g_{NR} = 1 + \frac{J(J+1) - L(L+1) + S(S+1)}{2J(J+1)} \quad (4)$$

helps to label the states with standard notations $^{(2S+1)}L_J$. Here the values of total spin (S) and orbital momentum (L) are chosen to fit the calculated values of the g-factors.

B. Calculation of transition probabilities and lifetimes

To determine the values of the transition probabilities (T) of the atomic states, we need to calculate the transition amplitudes (A). To do this, we use the time-dependent Hartree-Fock (TDHF) method, which is

equivalent to the random-phase approximation (RPA). A TDHF equation for the core can be written as follows:

$$\left(\hat{H}^{\rm RHF} - \epsilon_c\right)\delta\psi_c = -\left(\hat{f} + \delta V^f_{\rm core}\right)\psi_c. \qquad (5)$$

Here, $\hat{H}^{\rm RHF}$ is the RHF Hamiltonian (1), index c numerates states in the core, ϵ_c is the energy of electron state c, and ψ_c is the wave function of the state, $\delta\psi_c$ is a correction to the wave function due to the external field $\hat{f}$, $\delta V^f_{\rm core}$ is the correction to the self-consistent RHF potential of the core generated by the modifications to all core states in the external field.

After solving the RPA equations (5) self-consistently for finding $\delta V^f_{\rm core}$, the off-diagonal matrix element then gives the transition amplitude between valence states

$$A_{ij} = \left\langle \Psi_i \left| \hat{f} + \delta V^f_{\rm core} \right| \Psi_j \right\rangle \qquad (6)$$

Here, $|\Psi_i\rangle, |\Psi_j\rangle$ are the many-electron wave functions obtained by solving Eq. (3).

Once the transition amplitudes have been obtained, the transition probabilities can be determined using the following formulae (atomic units are assumed):

$$T^{M1}_{ab} = \frac{4}{3}(\alpha\omega_{ab})^3 \frac{A^2_{M1}}{2J_b+1}, \qquad (7)$$

$$T^{\rm E2}_{ab} = \frac{1}{15}(\alpha\omega_{ab})^5 \frac{A^2_{E2}}{2J_b+1}, \qquad (8)$$

We consider two types of transitions: magnetic dipole (T_{M1}) transition (7), and electric quadrupole (T_{E2}) transition (8). In both equations, α is the fine structure constant ($\alpha \approx \frac{1}{137}$), ω_{ab} is the energy difference between the lower (a) and upper (b) states, A is the transition amplitude (reduced matrix element) derived from Eq. (6), and J_b is the total angular momentum of the upper state b. Note that magnetic amplitudes A_{M1} contain the Bohr magneton μ_B ($\mu_B = \alpha/2 \approx 3.65\times10^{-3}$ in the Gauss-type atomic units).

The lifetime (in seconds) of the upper state b is given by

$$\tau_b = 2.4189 \times 10^{-17} / \sum_a T_{ab}, \qquad (9)$$

where the summation goes over all possible transitions to lower states a.

III. RESULTS AND DISCUSSIONS

A. Energy levels, g-factors, transition amplitudes, and lifetimes

We present the energy levels, g-factors and lifetimes of some states of the Sm^{10+} ion in Table I. First two long-living excited states are considered as clock states. The energies and g-factors are presented for 29 lowest even states with $1 \le J \le 8$. Odd states lie very high on the energy scale, $E > 170000$ cm^{-1}.

TABLE I. Excitation energies (E, cm^{-1}), g-factors, and lifetimes for low-lying states of the Sm^{10+} ion.

No.	Conf.	SLJ	Energy	g	τ
1	$5s^25p4f^3$	$^7J_5$	0.00	0.7469	
2	$5s^25p4f^3$	$^7I_4$	7882.62	0.7410	4.03 s
3	$5s^24f^4$	$^5I_4$	13139.18	0.6670	120.1 s
4	$5s^25p4f^3$	$^7J_6$	13290.72	0.9426	10.03 ms
5	$5s^25p4f^3$	$^1H_5$	16880.47	0.9711	31.84 ms
6	$5s^25p4f^3$	$^3I_7$	17214.24	1.1589	0.48 s
7	$5s^25p4f^3$	$^3F_2$	18525.27	0.6117	
8	$5s^25p4f^3$	$^7J_8$	19447.18	1.1825	
9	$5s^25p4f^3$	$^3I_7$	20337.14	1.1519	
10	$5s^24f^4$	$^5I_8$	20830.77	1.2413	
11	$5s^25p4f^3$	$^7I_6$	20979.87	1.1312	
12	$5s^24f^4$	$^5I_5$	23156.45	0.9092	
13	$5s^25p4f^3$	$^3D_1$	23203.75	0.6597	
14	$5s^25p4f^3$	$^3G_3$	24770.00	0.7638	
15	$5s^24f^4$	$^5I_6$	26355.12	1.0683	
16	$5s^25p4f^3$	$^1H_5$	26839.37	0.9644	
17	$5s^24f^4$	$^5I_7$	27056.60	1.1721	
18	$5s^25p4f^3$	$^7G_2$	27528.76	0.8476	
19	$5s^25p4f^3$	$^3G_3$	28247.93	0.8296	
20	$5s^25p4f^3$	$^3G_4$	28259.67	1.0888	
21	$5s^25p4f^3$	$^3S_1$	29073.92	2.0820	
22	$5s^25p4f^3$	$^3D_2$	29457.53	1.0945	
23	$5s^25p4f^3$	$^3G_4$	31509.39	1.0703	
24	$5s^25p4f^3$	$^1D_2$	32264.43	0.9642	
25	$5s^25p4f^3$	$^5G_4$	32323.63	1.1831	
26	$5s^25p4f^3$	$^5F_3$	32520.38	1.2525	
27	$5s^25p4f^3$	$^5H_5$	33467.08	1.1459	
28	$5s^25p4f^3$	$^3D_2$	33575.59	1.1598	
29	$5s^24f^4$	$^5F_1$	33694.72	0.1278	

As shown in Table II, we have calculated the transition amplitudes (A) and transition probabilities (T) for six low states of the Sm^{10+} ion. Since all low states have the same parity, only magnetic dipole (M1) and electric quadrupole (E2) contributions are significant. By using Eq. (9), we derived the lifetimes (τ) of the excited states using the transition rates from Table II.

B. Polarizabilities and blackbody radiation shifts

An important source of uncertainty in clock frequencies is blackbody radiation shift (BBR). To estimate this shift one needs to know static scalar polarizability ($\alpha_v(0)$) for both states of the clock transition.

The polarizability of state v can be expressed as a sum over a complete set of states connected to state v via the electric dipole (E1) transitions

$$\alpha_v(0) = \frac{2}{3(2J_v+1)} \sum_n \frac{A^2_{vn}}{\omega_{vn}}, \qquad (10)$$

TABLE II. Transition amplitudes (A, a.u.) and transition probabilities (T, 1/s) for some low states.

			(ω)		Present	
Transition	J_b	Type	[cm^{-1}]	[a.u.]	A [a.u]	T [s^{-1}]
2-1	4	M1	7882.62	0.0359	-1.50E-03	2.484E-01
2-1	4	E2	7882.62	0.0359	-0.2125	1.708E-05
3-1	4	M1	13139.18	0.0599	1.14E-04	6.637E-03
3-1	4	E2	13139.18	0.0599	-0.49522	1.194E-03
3-2	4	M1	5256.56	0.0240	1.19E-04	4.606E-04
3-2	4	E2	5256.56	0.0240	-0.85906	3.682E-05
4-1	6	M1	13290.72	0.0606	1.63E-02	9.675E+01
4-1	6	E2	13290.72	0.0606	0.35168	4.414E-04
4-2	6	E2	5408.1	0.0246	-0.43874	7.664E-06
4-3	6	E2	151.54	0.0007	-0.1065	7.801E-15
5-1	5	M1	16880.47	0.0769	2.22E-03	4.352
5-1	5	E2	16880.47	0.0769	-4.91E-02	3.361E-05
5-2	5	M1	8997.85	0.0410	1.42E-02	2.705E+01
5-2	5	E2	8997.85	0.0410	-2.38E-02	3.398E-07
5-3	5	M1	3741.29	0.0170	-8.92E-04	7.664E-03
5-3	5	E2	3741.29	0.0170	0.22821	3.883E-07
5-4	5	M1	3589.75	0.0164	-7.58E-03	4.895E-01
5-4	5	E2	3589.75	0.0164	-6.97E-02	2.948E-08
6-1	7	E2	17214.24	0.0784	4.16E-03	1.953E-07
6-4	7	M1	3923.52	0.0179	-1.60E-02	2.091
6-4	7	E2	3923.52	0.0179	-0.21774	3.288E-07
6-5	7	E2	333.77	0.0015	-3.01E-01	2.799E-12

TABLE III. Scalar static polarizabilities of the ground state, α_0(GS), and clock states, α_0(CS), and BBR frequency shifts for the clock transitions. $\delta\nu_{BBR}/\nu$ is the fractional BBR shift; ν is the clock transition frequency. The values presented for α_0(GS) and α_0(CS) include core and valence contributions. The value of the core polarizability is 0.246 a_B^3.

			$\Delta\alpha(0)$	BBR, (T= 300 K)		
Transition	α_0(GS)$[a_B^3]$	α_0(CS)$[a_B^3]$	α_0(CS) − α_0(GS)	$\delta\nu_{BBR}$[Hz]	ν[Hz]	$\delta\nu_{BBR}/\nu$
2 − 1	1.4603	1.4544	−0.0059	0.5081×10^{-4}	2.3631×10^{14}	2.150×10^{-19}
3 − 1	1.4603	1.7222	0.2619	-0.2255×10^{-2}	3.9390×10^{14}	-5.725×10^{-18}

where J_v is the total angular momentum of state v and ω_{vn} is the frequency of the transition. Notations v and n refer to many-electron atomic states. For the calculations of the polarizabilities of clock states, we apply the technique developed in Ref. [30] for atoms or ions with open shells. The method relies on Eq. (10) and the Dalgarno-Lewis approach [31], which reduces the summation in Eq. (10) to solving a matrix equation (for more details, see Ref. [30]).

A comparison of the polarizabilities of the ground and excited clock states is presented in Table III. The ground and the first excited clock state seem to have similar polarizabilities. The reason for this is that the frequency of the transition is small compared to the frequencies of the transitions to odd states ($E_{\rm odd} > 170000$ cm^{-1}). We have seen similar facts before in some other ions, see Refs. [32–34].

In atomic clocks, the BBR shift can considerably affect the frequency of the clock's transition. Its value in Hz is given by

$$\delta\nu_{\rm BBR} = -1.063\times10^{-12}T^4\Delta\alpha(0), \qquad (11)$$

where T is temperature (room temperature is T= 300 K) and $\Delta\alpha(0) = \alpha_0$(CS) − α_0(GS) is the difference between the excited and ground state polarizabilities given in atomic units. A summary of the BBR shifts for the clock states investigated in this work is presented in Table III. As can be seen, the relative BBR shifts for these transitions are among the smallest that have been examined so far, $\sim 10^{-19}$.

C. Quadrupole moments

The ground and clock states of the ion being considered have high values of total angular momentum (J=

TABLE IV. Quadrupole moment (Θ, a.u.) of the considered optical clock states.

No.	Conf.	LSJ	E (cm^{-1})	ME (a.u.) $\langle J\|\Theta_0\|J\rangle$	Θ
1	$5s^2 5p 4f^3$	$^7J_5$	0000	-0.3580	0.0820
2	$5s^2 5p 4f^3$	$^7I_4$	7882.62	-0.0611	-0.0145
3	$5s^2 4f^4$	$^5I_4$	13139.18	0.3950	0.0940

5 and 4). This makes them susceptible to the interaction between the gradient of the external electric field and the quadrupole moments of the states, which causes a frequency shift. Hence, it is crucial to have knowledge about the quadrupole moment values.

The quadrupole interaction Hamiltonian can be written as (see, e.g., Ref. [35])

$$H_{\mathcal{Q}} = \sum_{q=-1}^{1} (-1)^q \nabla\mathcal{E}_q^{(2)} \hat{\Theta}_{-q}, \tag{12}$$

where q is the operator component, and the $\nabla\mathcal{E}_q^{(2)}$ tensor represents the gradient of the external electric field at the position of the system. $\hat{\Theta}_q$ is the electric quadrupole operator (the same as for the E2 transitions) and describes as $\hat{\Theta}_q = r^2 C_q^{(2)}$, where $C_q^{(2)}$ is the normalized spherical function.

The electric-quadrupole moment Θ is defined as an expectation value of the $\hat{\Theta}_0$ operator,

$$\begin{aligned}\Theta &= \left\langle nJJ \left| \hat{\Theta}_0 \right| nJJ \right\rangle \\ &= \langle nJ\|\hat{\Theta}\|nJ\rangle \sqrt{\frac{J(2J-1)}{(2J+3)(2J+1)(J+1)}},\end{aligned} \tag{13}$$

where $\langle nJ\|\hat{\Theta}\|nJ\rangle$ denotes the reduced matrix element (ME) of the electric-quadrupole operator. In Table IV, the reduced ME of the electric quadrupole operators for the considered states are shown along with their Θ.

D. Sensitivity of the clock transitions to variation of the fine structure constant

The sensitivity of atomic transitions to α variation is calculated by writing the frequencies of the transitions in the following form

$$\omega(x) = \omega_0 + qx \tag{14}$$

Here ω_0 is the present laboratory value of the transition frequency and $x = (\alpha/\alpha_0)^2 - 1$, where α_0 is the physical value of α, q is the sensitivity coefficient, which can be determined by varying the value of α in computer codes and calculating numerical derivatives

$$q \approx \frac{\omega(+\delta) - \omega(-\delta)}{2\delta} \tag{15}$$

TABLE V. Sensitivity of the clock transitions to the variation of the fine-structure constant (q, K) of Sm^{10+}.

No.	Conf.	LSJ	ω (cm^{-1})	q(cm^{-1})	K
2	$5s^2 5p 4f^3$	$^7I_4$	7882.62	3100	0.79
3	$5s^2 4f^4$	$^5I_4$	13139.18	108700	16.5

To achieve linear behaviour, δ should be sufficiently small. On the other hand, it should be large enough to suppress numerical noise. In our case, we used $\delta = 0.01$ which leads to stable results.

To study possible variation of the fine structure constant one needs to measure frequencies of at least two atomic transitions over a long period of time. The ratio of changes in frequencies can be written as

$$\delta\left(\frac{\omega_1}{\omega_2}\right) / \frac{\omega_1}{\omega_2} = \frac{\delta\omega_1}{\omega_1} - \frac{\delta\omega_2}{\omega_2} \equiv (K_1 - K_2)\frac{\delta\alpha}{\alpha}. \tag{16}$$

The K parameter is known as the enhancement factor and has the formula $K = 2q/\omega$. It is clear that the highest sensitivity can be achieved if two atomic transitions have different sensitivity to the α variation. For both studied clock transitions, q and K have been calculated and are summarized in Table V. As one can see, the sensitivities of the transitions to α variation are different. For these two transitions Eq. (17) becomes

$$\delta\left(\frac{\omega_1}{\omega_2}\right) / \frac{\omega_1}{\omega_2} \approx 16\frac{\delta\alpha}{\alpha}. \tag{17}$$

For comparison, the highest sensitivity to α variation in working clocks can be found in the monitoring of the frequencies of E2 and E3 transitions in Yb^+, where $\Delta K \approx 7$ [36]. It may be convenient that the measurements for two frequencies can be done with the use of the same ion.

IV. SUMMARY

In this work we demonstrated that the Sm^{10+} ion has two metastable states which can be used to build atomic optical clocks with low sensitivity to perturbations and high sensitivity to the hypothetical time variation of the fine structure constant. Several atomic properties relevant to optical clock development have been calculated. These include energy levels, g-factors, lifetimes, electric quadrupole moments, BBR shift and sensitivity of clock frequencies to time variation of the fine structure constant. The relative value of the BBR shift is very small, $\sim 10^{-19}$. We found, that if fine structure constant α changes with time, the ratio of the two clock frequencies changes 16 times faster. This is significantly better than in best (in terms of sensitivity to α variation) operating atomic clocks based on the E3 and E2 clock transitions in the Yb^+ ion.

ACKNOWLEDGMENTS

S.O.A. gratefully acknowledges the Islamic University of Madinah (Ministry of Education, Kingdom of Saudi Arabia) for support. This work was supported by the Australian Research Council Grants No. DP230101058 and DP200100150.

[1] N. Ohmae, M. Takamoto, Y. Takahashi, M. Kokubun, K. Araki, A. Hinton, I. Ushijima, T. Muramatsu, T. Furumiya, Y. Sakai, *et al.*, Adv. Quantum Tech. **4**, 2100015 (2021).

[2] S. M. Brewer, J.-S. Chen, A. M. Hankin, E. R. Clements, C.-w. Chou, D. J. Wineland, D. B. Hume, and D. R. Leibrandt, Phys. Rev. Lett. **123**, 033201 (2019).

[3] N. Huntemann, C. Sanner, B. Lipphardt, C. Tamm, and E. Peik, Phys. Rev. Lett. **116**, 063001 (2016).

[4] W. McGrew, X. Zhang, R. Fasano, S. Schäffer, K. Beloy, D. Nicolodi, R. Brown, N. Hinkley, G. Milani, M. Schioppo, *et al.*, Nature **564**, 87 (2018).

[5] T. L. Nicholson, S. Campbell, R. Hutson, G. E. Marti, B. Bloom, R. L. McNally, W. Zhang, M. Barrett, M. S. Safronova, G. Strouse, *et al.*, Nature commun. **6**, 6896 (2015).

[6] N. Nemitz, T. Ohkubo, M. Takamoto, I. Ushijima, M. Das, N. Ohmae, and H. Katori, Nature Photonics **10**, 258 (2016).

[7] B. Bloom, T. Nicholson, J. Williams, S. Campbell, M. Bishof, X. Zhang, W. Zhang, S. Bromley, and J. Ye, Nature **506**, 71 (2014).

[8] T. Middelmann, S. Falke, C. Lisdat, and U. Sterr, Phys. Rev. Lett. **109**, 263004 (2012).

[9] A. D. Ludlow, W. F. McGrew, X. Zhang, D. Nicolodi, R. J. Fasano, S. A. Schaffer, R. C. Brown, R. W. Fox, N. Hinkley, T. H. Yoon, *et al.*, in *2018 Conference on Precision Electromagnetic Measurements (CPEM 2018)* (IEEE, 2018) pp. 1–2.

[10] C. Lisdat, S. Dörscher, I. Nosske, and U. Sterr, Phys. Rev. Res. **3**, L042036 (2021).

[11] J. Berengut, V. Dzuba, and V. Flambaum, Phys. Rev. Lett. **105**, 120801 (2010).

[12] J. Berengut, V. Dzuba, V. Flambaum, and A. Ong, Phys. Rev. Lett. **106**, 210802 (2011).

[13] J. Berengut, V. Dzuba, V. Flambaum, and A. Ong, Phys. Rev. Lett. **109**, 070802 (2012).

[14] M. Kozlov, M. Safronova, J. C. López-Urrutia, and P. Schmidt, Rev. Mod. Phys. **90**, 045005 (2018).

[15] M. G. Kozlov, M. S. Safronova, J. R. C. López-Urrutia, and P. O. Schmidt, Rev. Mod. Phys. **90**, 045005 (2018).

[16] Y.-M. Yu, B. K. Sahoo, and B.-B. Suo, Fronties in Physics **11**, 1104848 (2023).

[17] J. C. Berengut, D. Budker, C. Delaunay, V. V. Flambaum, C. Frugiuele, E. Fuchs, C. Grojean, R. Harnik, R. Ozeri, G. Perez, *et al.*, Phys. Rev. Lett. **120**, 091801 (2018).

[18] V. Flambaum, A. Geddes, and A. Viatkina, Phys. Rev. A **97**, 032510 (2018).

[19] C. Delaunay, R. Ozeri, G. Perez, and Y. Soreq, Phys. Rev. D **96**, 093001 (2017).

[20] V. Yudin, A. Taichenachev, M. Okhapkin, S. Bagayev, C. Tamm, E. Peik, N. Huntemann, T. Mehlstäubler, and F. Riehle, Phys. Rev. Lett. **107**, 030801 (2011).

[21] V. Dzuba, Phys. Rev. A **90**, 012517 (2014).

[22] V. Dzuba, J. Berengut, C. Harabati, and V. Flambaum, Phys. Rev. A **95**, 012503 (2017).

[23] V. Dzuba, Phys. Rev. A **71**, 032512 (2005).

[24] V. A. Dzuba, V. V. Flambaum, and M. S. Safronova, Phys. Rev. A **73**, 022112 (2006).

[25] V. V. Flambaum and J. S. M. Ginges, Phys. Rev. A **72**, 052115 (2005).

[26] W. Johnson and J. Sapirstein, Phys. Rev. Lett. **57**, 1126 (1986).

[27] W. R. Johnson, S. A. Blundell, and J. Sapirstein, Phys. Rev. A **37**, 307 (1988).

[28] V. Dzuba, V. Flambaum, P. Silvestrov, and O. Sushkov, J. Phys. B **20**, 1399 (1987).

[29] V. A. Dzuba, V. V. Flambaum, and M. G. Kozlov, Phys. Rev. A **54**, 3948 (1996).

[30] V. Dzuba, Symmetry **12**, 1950 (2020).

[31] A. Dalgarno and J. T. Lewis, Proc. R. Soc. A **233**, 70 (1955).

[32] S. O. Allehabi, V. Dzuba, and V. Flambaum, Phys. Rev. A **107**, 063103 (2023).

[33] S. O. Allehabi, V. Dzuba, and V. Flambaum, Phys. Rev. A **106**, 032807 (2022).

[34] S. O. Allehabi, S. Brewer, V. Dzuba, V. Flambaum, and K. Beloy, Phys. Rev. A **106**, 043101 (2022).

[35] W. M. Itano, J. Res. Natl. Inst. Stand. Technol. **105**, 829 (2000).

[36] V. V. Flambaum and V. A. Dzuba, Can. J. Phys. **87**, 25 (2009).